A new fractal-theory-based criterion for hydrological model calibration

Zhixu Bai[1], Yao Wu[1], Di Ma[1], Yue-Ping Xu[1]

[1]Institute of Hydrology and Water Resources, Civil Engineering, Zhejiang University, Hangzhou, 310058, China

Correspondence to: Yue-Ping Xu (yuepingxu@zju.edu.cn)

Abstract. Fractality has been found in many areas and has been used to describe the internal features of time series. But is it possible to use fractal theory to improve the performance of hydrological models? This study aims at investigating the potential benefits of applying fractal theory in model calibration. A new criterion named ratio of fractal dimensions (RD) is defined as the ratio of fractal dimensions of simulated and observed streamflow series. To combine the advantages of fractal theory with classical criteria based on squared residuals, a multi-objective calibration strategy is designed. The selected classical criterion is Nash-Sutcliffe efficiency (E). The E-RD strategy is tested in three study cases with different climate and geography. The results of experiment reveal that, from most aspects, introducing RD into model calibration makes the simulation of streamflow components more reasonable. Besides, in calibration, only little decrease of E occurs when pursuing better RD. We therefore recommend choosing the best E among the parameter sets whose RD is around 1.

Key words: fractal theory; Hausdorff dimension; multi-objective calibration; hydrological model

1 Introduction

Since the first hydrological model was developed, proper methods to evaluate the performance of models have been pursued by hydrological community and a large variety of criteria have been proposed and used over the years. Most of the criteria are based on the squared residuals or absolute errors (Pushpalatha et al., 2012). Krause et al. (2005) compared nine efficiency criteria including correlation coefficient (r^2), Nash-Sutcliffe efficiency (E), index of agreement (d) and their variants, but none of them show overall dominance. Kling-Gupta efficiency was developed by Gupta et al. (2009) and Kling et al. (2012) to provide a diagnostically interesting decomposition of the Nash-

Sutcliffe efficiency, which facilitates the analysis of the relative importance of its different components (correlation, bias and variability) in the context of hydrological modelling. Apart from criteria which are used to calculate model errors over the entire test period, there are also many criteria which focus on a certain period of interest. For example, criteria mentioned above are calculated over flood periods (Liu et al., 2017; Liu et al., 2019) or dry periods (Demirel et al., 2013). There are also literatures which calibrated hydrological models over different hydrological components other than streamflow, such as evapotranspiration (Pan et al., 2017), soil moisture (Gao et al., 2015), snow water equivalent and even glacier melt (Liu et al., 2019). Another approach to modify the performance of models is hydrological signature (Shafii et al., 2015). Nonetheless, uncertainties of hydrological signature simulation are often large (Westerberg and McMillan, 2015). Hao et al. (2013) proposed a method based on entropy theory for constructing the bivariate distribution of drought duration and severity with different marginal distribution forms. Pechlivanidis et al. (2014) combined conditioned entropy difference metric and Kling-Gupta efficiency for multi-objective calibration of hydrologic models. Li et al. (2010) used the Bayesian method for uncertainty assessment of hydrological model estimation. Chiew and McMahon (1993) classified calibration criteria into statistical parameters and dimensionless coefficients. Statistical parameters include mean value, standard deviation, coefficient of skewness, coefficient of variance and quantile points etc. Most of the dimensionless coefficients (include Pearson correlation coefficient (r^2), Nash-Sutcliffe efficiency coefficient (E) and Kling-Gupta efficiency coefficient etc.) are based on the squared residuals (Pushpalatha et al., 2012). According to squared-residuals-based coefficients' calculation formula, approaching of every simulated individual data to observed data makes the coefficients better.

Another deficiency of existing criteria is the preference of particular parts of hydrograph. For example, statistical parameters are easily influenced by extreme individuals and are with large uncertainties (Westerberg and McMillan, 2015). Coefficients provide a measure of the overall agreement between simulation and observation, but are still significantly influenced by particular parts of hydrograph. High flows make a significant contribution to the value of E and Kling-Gupta efficiency coefficient (Pushpalatha et al., 2012). Nevertheless, literatures report an underestimation of peak flow when using E as indicator alone (Jain and Sudheer, 2008). Overall, there is still large vacancy for calibration

55   criteria which can give consideration to individual data and whole hydrograph.

Since firstly introduced by Hurst in 1951, fractality of streamflow series has been studied for decades (Hurst, 1951). There has been a spectacular growth in fractal theory, which was expended to various areas and to multifractal theory (Bai et al., 2019; Davis et al., 1994). Following the fractal theory, descriptions of fractality include the Hurst exponent (rescaled range analysis) (Hurst, 1951), Hausdorff

60   dimension (box-counting dimension or local dimension) (Jelinek et al., 2008; Kenneth, 1990), and correlation dimension (Grassberger and Procaccia, 1983) etc. The difference of these dimensions is the calculation scheme of fractal dimensions, and they are numerically related. While the Hurst exponent calculated with rescaled range analysis was more widely used, the Hausdorff dimension could be expanded to multifractal analysis easily and has perspective applications in hydrology (Bai

65   et al., 2019; Zhou et al., 2014). The fractality of time series is generally considered as a reflection of self-affinity, periodicity, long-term memory and irregularity (Bai et al., 2019; Hurst, 1951; Mandelbrot, 2004). Self-affinity is a feature of a fractal whose pieces are scaled by different amounts in the x- and y-directions, and fractal dimensions represent the self-affinity of time series. The self-affinity of time series is the similarity of fine-resolution small parts and coarse-resolution large parts of data.

70   Hausdorff dimension is defined and calculated based on the self-affinity of data series. The periodicity and long-term memory of time series referred by its fractality are highly related. Long-term memory is the feature that the effect of an event in a series may persist for a relatively long time. Long-term memory of hydrological time series is usually studied with rescaled range analysis. The irregularity of a fractal series refers to the unpredictable changes in a time series, which is a feature of chaos

75   system. Generally, the Hausdorff dimension of streamflow series represents the magnitude of fluctuation, i.e., the fluctuations in river flow are large for large river flow and small for small river flow (Movahed and Hermanis, 2008). Such feature is also called as long-term correlation, which can be described with the Hausdorff dimension (Onyutha et al., 2019). However, applications of fractal theory in hydrology were limited in simple streamflow analysis, mostly only using the Hurst index

80   (Katsev and Lheureux, 2003). Also, some literatures mentioned other indices based on fractal theory (Bai et al., 2019; Yu et al., 2014; Zhang et al., 2010), but again, the research objects were only observed hydrological data. Recent literatures made a progress to hydrological modelling based on fractal

theory (Zhang et al., 2010), but the model only reconstructs flood/drought grades series. As demonstrated by all these literatures, the fractality of observed streamflow series (as well as other hydro-meteorological data) is inherent and represents some peculiarity of their study cases. However, few literatures have tried to explore the applications of fractal theory in hydrological model calibration. To our best knowledge, the only exception is Onyutha et al. (2019), who utilized Hurst-Kolomogorov framework to evaluate the performance of climate models (GCM and RCM) rather than to calibrate hydrological models. In their study, Hurst exponent was used to represent the long-range dependence and evaluate the reproductivity of variability (Onyutha et al. 2019). However, the benefits of using fractal theory in model building and calibration have not been discussed.

Unlike typical statistical evaluation of fluctuation (such as standard deviation and distribution function), the Hausdorff dimension takes the order of data into account. Therefore, on the basis of classical criterion comparing observed and simulated water balances, the Hausdorff dimension can offer useful insight into mechanisms controlling the extreme hydrological events (including floods, droughts and low flows) (Radziejewski and Kundzewicz, 1997). Another difference between fractal dimension and classical criteria is the influence of individual (or a small number of) data. While approaching of every simulated individual data to observed data makes the coefficient better, it may make the Hausdorff dimension of simulated data closer or farther away from that of observed data. Given all that, the Hausdorff dimension is proposed in this study in hydrological model calibration. A good hydrological model shall be able to reproduce the streamflow well in all aspects, which means simulated streamflow series and observed streamflow series have similar Hausdorff dimensions.

Since the fractal dimension describes the fractality of streamflow series and two different series may have the same fractal dimension, the fractal dimension could not be used to calibrate hydrological model independently. Multi-objective optimization approaches are widely used by hydrological community (Harlin, 1991; Yapo et al., 1998; Liu et al., 2017; Liu et al., 2019; Pan et al., 2017; Shafii et al., 2015; Ye et al., 2014). This set the stage of using some uncomprehensive but effective criteria as targets, such as aforementioned hydrological signatures (Shafii et al., 2015; Westerberg and McMillan, 2015), statistical targets and fractal criteria. Nonetheless, the strategy to use Hausdorff dimension to calibrate hydrological models has not been studied.

In this study, a new criterion defined as ratio of fractal dimension (RD) is introduced, as well as a calibration strategy. The criterion and calibration strategy should be able to consider the self-affinity, periodicity, long-term memory and irregularity of hydrograph during model calibration. Three catchments with different climate and geography are used as case studies. The aim of this study is to examine the applicability of using RD as one of the targets of multi-objective calibration and explore the performance of hydrological models when RD is considered. Section 2 describes differences between RD and classical criteria and how RD is used in calibration (E-RD strategy). Section 3 contains the brief information of study areas and methods used in this study to investigate the advantages of RD. Section 4 provides the results and Section 5 provides the discussion. Section 6 is the summary and conclusion. In this study, our goal is to answer the following questions: (1) Is RD a proper criterion for hydrological modelling, even if the reflection of RD is not as direct as classical criteria? (2) Could E-RD strategy explicitly improve the performance of hydrological models? (3) Why can RD be used to improve calibration?

2 Study area and methodology

2.1 Ratio of fractal dimensions and E-RD strategy

The box-counting method used to calculate Hausdorff dimension is based on the idea of separating data into boxes and count the number of boxes (Mandelbrot, 2004). When adopted to analysis of time series, the box-counting method sums adjacent data up (put adjacent individuals into boxes) and compares the treated data of various resolutions (different sizes of boxes). Fig. 1 graphically shows how the box-counting method works with time series. Fig. 1 (a) shows how the number of boxes needed to cover all data (N) changes when the size of boxes changes (resolution, δ). Fig. 1 (b) shows the log-linear relationship between N and δ. The definition of Hausdorff dimension D is:

$$D = \frac{\log (\mathrm{N})}{\log (1/\delta)}, \tag{1}$$

Where δ is the size of boxes and N is the number of boxes (Evertsz and Mandelbrot, 1992).

Fig. 1. Flow chart of using box-counting method to calculate the Hausdorff dimension of time series.

As stated before, the observed and simulated streamflow series shall have the same Hausdorff dimension. In this study, a new criterion named as ratio of dimension (RD) is defined as follow:

140 $$RD = \frac{D_s}{D_o},\qquad\qquad\qquad (2)$$

where D_s is the Hausdorff dimension of simulated streamflow series and D_o is the Hausdorff dimension of observed streamflow series. The range of RD is from 0 to $+\infty$. When $RD=1$, the simulated streamflow series has the same Hausdorff dimension with that of observed streamflow series, which means that the model is the best in terms of fractals. The relevant examination of models'

145 performance under the supervision of RD has not been studied, either.

Obviously, RD, as a metric of self-affinity deviation of simulated streamflow series from observed series, is not a criterion capable of evaluating the performance of hydrological models by itself. An immediate thought is to combine RD and another statistical criterion in model calibration.

Three features are demanded for the statistical criterion to be combined with RD. Firstly, the statistical

150 criterion shall be able to evaluate the performance of models in terms of water balance to some extent. Secondly, the statistical criterion shall evaluate the response of streamflow to meteorological forcing. Thirdly, the criterion shall calculate model errors over the entire test period. These features make sure that the strategy meets basic needs. An additional requirement for the statistical criterion used in this study is the popularity of this criterion within the hydrological community. Another reason to choose

155 E in our study is that the pros and cons of E are more familiar for hydrologists than other metrics, and this original version is still mostly often used in hydrological model calibration. In this manner, the advantages of RD emerge as well as the benefits of multi-objective calibration based on RD.

Nash-Sutcliffe efficiency coefficient (E), a commonly used criterion since initially proposed (Jain and Sudheer, 2008; Nash and Sutcliffe, 1970), is selected in this study. The calculation of E is:

160 $$E = 1 - \frac{\sum(Q_o - Q_s)^2}{\sum(Q_o - \overline{Q_o})^2},\qquad\qquad (3)$$

Where Q_s is the simulated flow, Q_o is the observed flow, $\overline{Q_o}$ is the mean value of the observed flow.

A set of experiments is processed to illustrate the benefits of using the proposed $E\text{-}RD$ strategy to evaluate models. Descriptions of experiments are included in Section 3. Fig. 2 shows the whole

165 process of $E\text{-}RD$ strategy.

Fig. 2. Flow chart of *E-RD* strategy.

The value of Hausdorff dimension of the same time series may be different for different resolution.
170   The difference usually implicates that self-affinity of the time series changes as the resolution changes
and in hydrology specifically, dominant driver of hydrological processes changes. For example, the
dominant drivers of daily and annually circle of temperature are different. Hausdorff dimension helps
reveal the dominant drivers of hydrological process (Bai et al., 2019). According to this idea,
Hausdorff dimension determines whether the streamflow components are reasonably simulated. In
175   this study, the largest temporal resolution is set as 365 days (1 year), to leave the inter-annual drivers
out. It is believed that the range of resolution is enough for Hausdorff dimension to reflect drivers of
hydrological processes.

2.2 Study area

A small catchment located in Tibet named Dong, a medium sized catchment located in southeastern
180   China named Jinhua and a large catchment located in the middle reach of Yangtze River named Xiang
are used in this study.

Dong is a small tributary of the Yarlung Zangbo River, with elevation ranging from 3512 to 5869 m.
The area of Dong catchment is about 43.6 km^2. The average annual precipitation of study period is
413.5 mm. The average temperature is 10.6 ℃. The high elevation of Dong catchment results in cold
185   climates. Former study has consolidated that snow pack and frozen soil significantly effect
hydrological processes in the Dong catchment (Bai et al., 2019). Meteorological forcing data and
streamflow observation of Dong catchment used in this study are from 2011 to 2014.

Jinhua River is a 5536-km^2 catchment of Zhejiang Province, southeastern China. The study area is
subject to Asian monsoon climate, and precipitation is strongly summer-dominant, occurring mostly
190   from May to September. Based on meteorological data of 42 years (from 1965 to 2006), the mean
annual precipitation in Jinhua catchment is 1847.4 mm. The average temperature is 17.6 ℃. Former
studies show that precipitation data and streamflow data of Jinhua catchment are well matched (Pan
et al., 2018). Meteorological forcing data and streamflow observation of Jinhua catchment used in this

study are from 1965 to 2006.

195   Xiang River is one of the largest tributaries of the Yangtze River, which flows into the Dongting Lake,

the second largest freshwater lake in mid-China. The area of Xiang catchment is about 82,400 km^2

and data of nine meteorological stations are used in this study. Dominated by subtropical monsoon

climate, the mean annual rainfall of the basin ranges from 1400 to 1700 mm and the average annual

temperature is around 17 ºC. The basin experiences floods and droughts frequently, and rainfall is

200   distributed evenly throughout the year, most of it falling in April to June. According to literatures,

precipitation is the most vital driver for Xiang River (Zhu et al., 2019). Meteorological forcing data

and streamflow observation of Xiang catchment used in this study are from 1987 to 2013.

Fig. 3 shows the topography of all study areas.

205   Fig. 3. DEM of study areas.

2.3 HBV model

The HBV model is a conceptual rainfall-runoff model originally developed by Swedish

210   Meteorological and Hydrological Institute (SMHI) (Bergström, 1976; Bergström, 1992; Lindström et

al., 1997). The model has been successfully used in many cases (Seibert and Vis, 2012; Tian et al.,

2015; Tian et al., 2016). The HBV model is composed of precipitation and snow accumulation routines,

a soil moisture routine, a quick runoff routine, a baseflow routine and a transform function. The HBV

model takes into account the effect of snow melting and accumulation, which is significant in the

215   Dong catchment. The actual evapotranspiration is calculated with a linear function. Two conceptual

runoff reservoirs, the upper reservoir and the lower reservoir are included in HBV model.

2.4 Multi-objective genetic algorithm

A controlled, elitist genetic algorithm (a variant of NSGA-II) (Deb, 2001) is applied in model

calibration. A controlled elitist GA favors individuals with better fitness value (rank) as well as

220   individuals that can help increase the diversity of the population even if they have a lower fitness

value. An important behavior of this genetic algorithm is, the individual with the best performance according to anyone of the criterion would be retained with the lowest rank. This makes sure that with multi-objective genetic algorithm, parameter set with the best possible E could be found and the following comparison between RD-E and E is reasonable. In this study, $|1 - RD|$ is used as one of the criteria.

Since HBV has 14 parameters to calibrate, the number of generations is 2800. Each generation has 600 population. The crossover fraction is set as 0.8 (meaning). The Pareto fraction is set as 0.2 (meaning). The population migrates every 20 generations, and the migration fraction is set as 0.5. These settings make sure that population will not trap in local optimum, which is important because RD varies in a wider range than traditional criteria. Most of these numbers are the default settings, which is applicable to most of the questions. Only the number of the population of each generation (600) is larger than default (200) for finer presentation of Pareto front of the optimization. The meanings of settings can be found in Deb (2001).

All 600 Pareto-optimized solutions of the last generation are used in the following analysis. GA optimization with the E-RD calibration strategy (described in 2.2) will not drop population with perfect RD (=1) and unsatisfactory E. Several representative selected parameter sets and corresponding simulated streamflow series are deeply studied.

2.5 Approach for model evaluation

To investigate the RD's effects in hydrological model evaluation, several tools are utilized. Pearson's correlation coefficient r^2, percentage bias (bias), auto-correlation of observation, auto-correlation of simulation, relative variance, maximum monthly flow and minimum monthly flow are used for a comprehensive comparison between models based on RD and traditional hydrological criteria (E). The best RD model and best E model (typical models) are selected from the last generation of GA calibration for detailed analysis.

To understand how the model is adjusted when RD is used as one of the objectives, the relationship between parameters and RD is analyzed. The distance correlation r_d^2 is used to determine whether the variations of model's parameters and RD are related. The distance correlation, as a multivariate measure of dependence, calculates the correlation of distances between points to means. The distance

correlation is believed to have better performance when solving problems with non-linear data or extreme values (Székely, Rizzo and Bakirov, 2007). The relationship between parameters and RD may not be linear, which brings the necessity of using a nonlinear analysis approach rather than Pearson's linear correlation coefficient. Distance correlation is also more robust to data outliers, than rank correlations.

To look into the influence on simulation of specific parts of hydrological hydrographs brought by RD, fast flow and baseflow are analyzed separately. The HBV model is slightly modified to output simulated fast flow and baseflow at every time step. Observed streamflow series are divided into the fast and baseflow using the Water Engineering Time Series PROcessing tool (WETSPRO tool) introduced by Willems (2009). WETSPRO separates fast flow and slow flow on the basis of filter theory, using several filter parameters including recession constant, average fraction of fast flow volumes over the total flow volumes, etc. The E and r^2 of simulated fast flow/baseflow to observed fast flow/baseflow are calculated. Hydrographs of the first three years after warming up are shown to visually illustrate the influence of RD on fast flow and baseflow simulation.

3 Results and discussion

3.1 Overall evaluation of models on the Pareto front

Fig. 4 shows the RD-E relationship of last population of multi-objective calibration in three catchments separately. The ranges of RD of final generation in three cases are different, so as the ranges of E/bias. The ranges of E are 0.60 to 0.69 (Dong), 0.95 to 0.953 (Jinhua) and 0.818 to 0.822 (Xiang). For all cases, the non-significant variation of E indicates that for all selected parameter sets, the E criteria could not fully distinguish them. On the contrary, the ranges of RD are about 0.72 to 1 (Dong), 0.86 to 1.04 (Jinhua) and 0.85 to 1.01 (Xiang). According to literatures, the biggest difference of Hausdorff dimension of data of the same type is smaller than 0.25 (Hurst, 1951; Rubalcaba, 1997; Meseguer-Ruiz et al., 2019), which indicates the ranges of RD aforementioned are well marked. In this study, RD is often lower than 1 and sometime only slightly higher than 1, which should be the result of smooth hydrograph and simple structure of HBV model. Because that RD=1 means that the model is best in terms of fractals (see Section 2.2), the models whose RD is larger

than 1 need discussion, too. Noting that the largest RD is very close to best RD (=1), the largest

RD model should be similar with the best RD model. And the GA algorithm discards most of the

models with $RD > 1$ because they are not on the Pareto front. The bias does not change much when

RD changes. A tiny difference within 3% occurs for the last generations of Dong, Jinhua and Xiang.

280   More importantly, change of bias with the change of RD is different for three cases. For Dong

catchment, the bias is firstly getting worse then getting better as RD approaching 1. Besides, a trend

of bias of getting worse for Jinhua and a trend of bias of getting better for Xiang as RD approaching

1 can be observed. Without more cases, the trend of bias in this study is regarded to be random. In

addition, in Xiang case, there is a break in Fig. 4. On two sides of the break, E is close by and RD

285   is significantly different.

A single-objective calibration was operated to support the assumptions made in Section 3.3 that, in

this study, the NSGA II algorithm could find the best E. The comparison between results of single-

objective calibration and multi-objective calibration (E-RD strategy) is listed in Table 1. Besides, to

get rid of the possible influence of the lengths of time series, a comparison of the multi-objective

290   calibration with the same length of data is made. The results show that, at least in the cases of this

study, the E-RD strategy would not change its behavior with the lengths of data.

Fig. 4 E-RD of last generation of GA calibration.

295   Table 1. Comparison of best E between single-objective calibration and multi-objective calibration

(E-RD strategy).

The models with the best RD, best E and largest RD are selected from Pareto front as typical

examples. Fig. 5 is the simulated streamflow of three examples and observed streamflow as well. For

300   each case, discharge within a three-year period is shown. Examples with the largest RD are used to

verify if the model with the same RD with observation is the best. Apparently, the simulated

hydrographs of typical models in each case are similar, which agrees with the E and RD in Fig. 4.

Fig. 5. Typical examples with best RD, best E and largest RD (representative three-year hydrograph).

A precondition of adopting the RD-E strategy is the irrelevancy or weak correlation between two criteria. This precondition could be simply verified by looking into their calculation schemes or by examining during the multi-objective calibration. In this study, the former is apparent and the latter is conducted and briefly shown in Fig. 4. The best E and worst E are close according to the result of multi-objective calibration. Figs. 4 and 5 further implicate that only little decrease of E happens when pursuing better RD. In this study, the equifinality of using only E emerges.

Table 2 lists the E values of typical models selected by the E-RD calibration strategy and optimized model. Table 2 confirms the assumption that, in this study, directly analyzing the models calibrated by E-RD calibration strategy is reasonable and efficient. Hydrological signatures including relative variance, lag-1 auto-correlation, percentage bias and maximum/minimum monthly flow are used to show the effect of RD.

Table 2. Hydrological signatures of typical models in all three cases.

Table 2 shows the hydrological signatures of observed and simulated flow series in three cases. Most hydrological signatures, including lag-1 auto-correlation, relative variation and maximum monthly flow, of simulated series are close by. Lag-1 auto-correlations of simulated series are close with auto-correlations of observed flow series. The lag-1 auto-correlations of series of flow series in Dong case and Xiang case are more than 0.9 while the values in Jinhua case are between 0.75 to 0.77. The relative variances of flow series in Dong case and Xiang case are smaller than 1, while the values in Jinhua case are more than 1.8. These show the feature of catchments of different types which are well simulated by the HBV model. Maximum and minimum monthly flows of simulated and observed series are significantly different. In all three cases, maximum monthly flows of simulated series are close to each other and slightly smaller than maximum monthly flows of observed flow series. Minimum monthly flow is the only hydrological signature used in this study that distinguishes the

typical models with the best RD and with the best E. In all three cases, the minimum monthly flow of simulated series with the best E is significantly smaller than of the minimum monthly flow observed series. On the contrary, the minimum monthly flow of simulated series with the best RD is close to the minimum monthly flow of observed series in Jinhua and Xiang cases. The minimum monthly flow of simulated series with the largest RD is worse than that of simulated series with the best RD. The high-flow percentiles (Q_5) and low-flow percentiles (Q_{75}) are reasonable in three cases for all typical models. However, the high-flow percentiles and low-flow percentiles of best RD models are still closest to the observation. In summary, hydrological signatures illustrate that major effects of RD are on the model's low flow simulation. Therefore, in later sections, low flow related analysis will be more emphasized.

3.2 Effect of RD on model parameters

All parameter sets in the Pareto front of three cases vary. The distance correlations (r_d^2) of parameters and RD are used to determine whether the change of parameters is stable. In addition, high value of r_d^2 indicates the significant relationship between Hausdorff dimension and these parameters. In this study, the relation between GA-selected parameter sets and E is not shown because E and RD in the Pareto front are highly related and the variance of E is small (see Fig. 4).

Table 3 lists the determinative parameters of three cases respectively. Distance correlation (r_d^2) is used to illustrate the non-linear relationship between E and RD in the Pareto's optimal. The parameter effective precipitation exponent (β) and degree-day factor are also listed in Table 3. Effective precipitation exponent is listed in Table 3 because of two reasons: 1) the range of r_d^2 of β in Jinhua case is from 0.709 to 0.739 in Xiang case, which is better than all unlisted parameters; 2) β, as well as determinative parameters α, KF, KS, is a runoff-generation-related parameter. The degree-day factor is listed in Table 3 because of two reasons: 1) distance correlation between the degree-day factor and RD is close to 0.8 in Xiang case; 2) in Dong case, distance correlation analysis does not show the significance of ablation of snow to hydrograph. Capillary transport is not determinative parameters to RD in Dong and Jinhua and therefore no further discussion of them is given afterwards. The r_d^2 of β (0.512) in Dong catchment is smaller than those in other cases. Fig. 6 shows the relationship between β and RD.

360

Table 3. Determinative parameters and distance correlations (r_d^2) between parameters and RD.

*: $r_d^2 \geq 0.8$

365 Fig. 6. β and RD relationship in three cases.

An explicit relationship between parameters and criteria confirms that the effect of RD is not random.

Six parameters (β, α, fast flow factor, baseflow factor, percolation, degree-day factor) are selected by

distance correlation analysis for further discussion.

370 Fig. 7 shows the relationship between α and RD. The fast flow factor (KF) is related to RD in all

cases. Fig. 8 shows the relationship between KF and RD. The varying patterns of α and KF are the

same in three cases. The fast flow exponent α increases when RD approaches to 1 and KF decreases

when RD approaches to 1.

375 Fig. 7. α and RD relationship in three cases.

Fig. 8. KF and RD relationship in three cases.

Fig. 9 shows how fast flow changes with different surface water storages under different KF and α

380 of example models with best RD and best E. For all cases, E selects higher KF and lower α. In

Dong case, the relative difference of fast flow generation between best RD model and best E model

is always around 36%. The difference of fast flow between best RD model and best E model is

significant in Dong case for the whole simulated period. In Jinhua case, the relative difference between

the best RD model and best E model decreases from more than 20% to less than 5%. In Xiang case,

385 the relative difference between the best RD model and best E model decreases from about 16% to

8%. The difference between the best RD model and best E model is important during the dry period

and reduces as water storage of upper reservoir increases (the wet period). The relative difference is

greater in Jinhua case than in Xiang case in low flow period but smaller in Jinhua case in high flow period. That difference between the best E model and best RD model will finally lead to the greater variation of fast flow in low flow period than in high flow period. There are break points in Xiang case (Fig. 6, 7 and 8), but no evident effects shown in Fig. 5 and 9.

Fig. 9. Response of fast flow to surface water storage. For each case, fast flow responses of typical models with best RD and E are presented.

The baseflow (slow flow) factor (KS) is related to RD in all cases. Fig. 10 shows the relationship between KS and RD. The varying patterns of KS are the same in three cases. However, the variation ranges of KS in three cases are different. The largest value of KS in Dong (0.153) is much larger than that in Jinhua (0.063) and in Xiang (0.048). The smallest value of KS in Dong (0.016) is also larger than that in Jinhua (0.005) and in Xiang (0.010). The KS of best-E in the three cases follows the sequence of catchment area. This agrees with the regular pattern that the concentration time of slow flow is highly related with the area of catchment.

Fig. 10. KS and RD relationship in three cases.

The percolation is significantly related to RD in all cases. The range of percolation in Dong case is larger than the others. Fig. 11 shows the relationship between percolation and RD in three cases. Percolation increases in Dong case and decreases in other two cases when RD increases. The range of percolation in Dong is larger than in the others. KS and percolation determine the way the HBV models baseflow. The percolation in Dong case is larger than the others, which is the reflection of Dong catchment's arid climate. The percolation in Jinhua case is larger than the percolation in Xiang case, because the slope in Jinhua catchment is larger.

Fig. 11. Percolation and RD relationship in three cases.

The degree-day factor is significantly related to RD in Xiang case. However, the relationship between the degree-day factor and RD in Dong and Jinhua is weak. Fig. 12 shows the relationship between the degree-day factor and RD. The degree-day factor of most selected models of Dong case is smaller than 0.05, indicating that these models barely have any snow-melt runoff. When $RD>0.9$,

420   several models have degree-day factors larger than 7. When RD is around 1, the range of degree-day factor is 8.18 to 11.76, indicating that RD somehow detects the snow-melt runoff in the hydrograph and makes the HBV model simulate the snow-melt runoff more reasonably. Notably, the RD-selected degree-day factor in Dong case is too large according to the guidance of HBV (1.5 to 4 mm/day, in Sweden) (Seibert, 2005), which may result from the unsuitable lumped model structure of HBV in

425   rugged mountainous catchment.

The degree-day factor in all selected models of Jinhua is large, but the temperature in Jinhua is too high to have snow accumulation. The distance correlation between the degree-day factor and RD is weak in Dong and Jinhua case. The range of degree-day factor of most models in Xiang case is from 2.8 to 3.4. The range is small and so as the difference of snow-melt runoff of selected models. By

430   checking the temperature series in the Xiang catchment, we find there are 61 days (out of 27 years) when the average temperature is below 0°C. Actually, since the Xiang catchment is large, there are snow events somewhere in the catchment almost every year. The low temperature may be covered by the averaging, but the E-RD strategy captured it and illustrate this by noticeable value of degree-day factor.

435

Fig. 12. Degree-day factor and RD relationship in three cases.

As illustrated in Fig. 7, 8, 10 and 11, the three runoff-generation-routine parameters, namely baseflow factor (KS), fast flow factor (KF) and fast flow exponent (α), have the same change patterns in three

440   cases, suggesting a consistent preference of RD in all cases. Fig. 9 shows the visual difference of fast flow caused by introducing RD. However, other parameters have different change patterns along with RD because of different features of catchments (Fig. 6 and 12). For example, the soil parameter β, as illustrated by Equation (6), redistributes the precipitation and divides it into effective precipitation

and infiltration. β in Dong case and Xiang case increases and β in Jinhua decreases when RD is
getting better.

3.3 Analysis of separated streamflow

Separated simulated and observed streamflow series further reveal how RD influences model
calibration results. The simulated total flow is also separated with the WETSPRO tool to make the
principle of separation of simulation and observation same. Table 4 lists the parameters of WETSPRO
in three cases. The recession constants are close to each other. The w-parameter filter, representing the
case-specific average fraction of the quick flow volumes over the total flow volumes, shows the
difference. The w-parameter filter of Dong catchment is 0.14, smaller than the other catchments,
meaning that less proportion of total flow in Dong is baseflow, showing the catchment features of
small area and high slope. Fig. 13 shows the correlation coefficients between simulated and observed
fast flow/baseflow (r_f^2 and r_b^2) and Nash-Sutcliffe efficiency coefficient (E_f and E_b) of all
population of last generation in three cases and their variation with RD. The observed fast flow and
baseflow are separated from observed total flow using WETSPRO (William, 2009) (see Section 3.4).
In Dong case, both r_b^2 and r_f^2 slightly decrease as RD approaching 1. However, the range of r_f^2
in Dong case is from 0.02 to 0.15 and the range of r_b^2 is from about 0.3 to 0.6, which means no
correlation exists between simulated and observed fast flow and baseflow. The E_f and E_b in Dong
case improve to 0.06 and 0.24 respectively. In Jinhua and Xiang cases, all models of last generation
of GA simulate fast flow well. The r_f^2 and E_f value in Jinhua case are above 0.95 and 0.94. The r_f^2
and E_f in Xiang case are above 0.78 and 0.70. Surprisingly, there is still an evident improvement of
fast flow simulation due to the application of RD. The major improvement is the performance in
baseflow simulation. The values of criteria of baseflow simulation (r_b^2 and E_b) are improved from
poor to satisfactory. In Jinhua case, r_b^2 is improved from less than 0.1 to more than 0.45 and E_b is
improved from -10 to about 0.38. In Xiang case, r_b^2 is improved from about 0.4 to 0.75 and E_b is
improved from -6 to 0.51.

Fig. 13. Correlation coefficients and Nash-Sutcliffe efficiency coefficients on fast flow and baseflow
respectively of models of last generation in three cases.

Fig. 14 and 15 show separated streamflow of typical models and observed streamflow to make a visible comparison of models based on E and models based on RD. Fig. 14 shows the fast flow and Fig. 15 shows the baseflow.

Fig. 14. Fast flow of typical models and observations (representative three-years hydrograph).

Fig. 15. Baseflow of typical models and observations (representative three-years hydrograph).

The fast flow response of the best RD model in Dong case matches well to observed fast flow. The recession of fast flow of the best RD model in Dong case is too fast and the stable value is nearly zero, which is in the contrast of observation. The fast flow response of best E model in Dong is late, the recession of fast flow is too slow and fast flow at recession periods is too much. The fast flow response of largest RD model in Dong is also late, but the fast flow recession is more reasonable. In Jinhua and Xiang cases, simulated fast flow of all typical models well matches the observation. In all cases, the fast flow of best RD model is smaller than that of best E model and the difference is greater in low flow periods, which is consistent with Fig. 9.

In all three cases, the best RD models simulated baseflow well. RD selected models accurately simulated the seasonal flow variation of three catchments. The amplitude of baseflow fluctuation is close to separated observation by WETSPRO. The discharge also fits separated observation well. In all three cases, best E models do not simulate the baseflow well enough. The models with the largest RD in three cases have different performance. Dong-largest RD model, of which $r_b^2 = 0.82$ and $E_b = 0.25$, is not satisfactory. On the contrary, r_b^2 and E_b of the best E model in Dong are 0.87 and 0.79 respectively. The best E models in Jinhua and Xiang case, however, are close to the best RD models. According to Fig. 10 and 11, in Jinhua and Xiang cases, smaller KS and percolation (of best RD model) make smaller recharge and outflow (baseflow) of lower reservoir and smaller fluctuation of baseflow. In Dong case, bigger percolation increases the recharge and total baseflow and smaller KS extends the period of baseflow recession, making simulated baseflow more consistent

500   with observation (Fig. 15).

Two reasons exist for the unsatisfactory simulation of fast flow in Dong case. The first one is that the HBV model is not capable to accurately simulate mountainous catchment with snowpack and little gauge data are available for the Dong catchment. The second one is that WETSPRO may fail to correctly separate the short streamflow series of Dong catchment. This needs to be further verified.

505   Another visual demonstrator of the preference of RD is Fig. 14 and 15. Fast flow generation based on RD is more immediate while baseflow generation based on RD is smoother. Both of them are visually better than that when RD is not taken into account.

Above results reveal the benefits of using RD and the slight decrease of E. The selection principle based on multi-objective calibration is therefore suggested following two steps: 1) sieving out all

510   parameter sets whose RD is around 1 (in this case, considering the data precision of MATLAB, RD =1); 2) Choosing the parameter set with best E among the sets in Step 1. It is determined that the E-RD strategy using this selection principle improves the reliability of streamflow components simulation.

That is, RD selects responsive fast flow (confirmed in Fig. 14) and smooth baseflow (confirmed in

515   Fig. 15) in all cases.

4 Conclusion

This study targeted at examining the possibility of using fractal theory to improve the performance of hydrological models. The definition of ratio of fractal dimension (RD) was proposed and used as a fractal criterion (against traditional statistical criteria). A scheme which combined RD and Nash-

520   Sutcliffe efficiency coefficient (E) to calibrate hydrological models was developed and examined. Three study cases named Dong, Jinhua and Xiang were included in the examination. This is the first time (to our best knowledge) that fractal theory was applied to calibrate hydrological models.

Here are the main conclusions of this study:

1) The varying patterns of parameters of runoff generation routine (namely fast flow factor, fast flow

525   exponent and baseflow factor) are similar in all cases of our study.

2) Several parameters were found related to RD in specific cases as a result of specific characteristics

of study areas. For instance, $E\text{-}RD$ strategy selected the degree-day factors with relatively high value in Dong case, which is not seen when only E was considered.

3. The $E\text{-}RD$ strategy is innovative in hydrological modelling. That is, the $E\text{-}RD$ calibration strategy is a potential way to take the fractality of observed streamflow series into model calibration. Since fractal (also regarded as self-affinity) widely exists in nature and fractal of streamflow series is substantial, the RD as a criterion can be a good supplement for hydrological model calibration.

The $E\text{-}RD$ strategy introduced here needs more case studies to corroborate its capability further. The combination of other traditional statistical criteria and RD shall also be examined. More studies are also needed to dig out more benefits of applying fractal theory in hydrological modelling.

Acknowledgement

This study is financially supported by National Key Research and Development Plan "Inter-governmental Cooperation in International Scientific and Technological Innovation" (2016YFE0122100), the Natural Science Foundation of Zhejiang, China (LZ20E090001) and National Natural Science Foundation of China (91547106). The authors are indebted to PowerChina Huadong Engineering Corporation Limited, who provided meteorological and hydrological data in Dong catchment. National Climate Center of China Meteorological Administration is greatly acknowledged for providing meteorological data in the Jinhua and Xiang catchments, and Zhejiang Hydrological Bureau is acknowledged for providing hydrological data in the Jinhua River.

Reference

Abebe, N., A., Ogden, F., L. and Pradhan, N., R.: Sensitivity and uncertainty analysis of the conceptual HBV rainfall–runoff model: Implications for parameter estimation. J. Hydrol. 389(3-4): 301-310, 2010.

550   Bai, Z., Xu, Y. P., Gu, H. and Pan, S.: Joint multifractal spectrum analysis for characterizing the nonlinear relationship among hydrological variables. J. Hydrol., 576, 12-27, 2019.

Bergström, S.: Development and application of a conceptual runoff model for Scandinavian catchments. SMHI Report RHO NO. 7, Norrköping, Sweden, 1976.

Bergström, S.: The HBV model - its structure and applications. SMHI Reports RH NO. 4, Norrköping,

555   Sweden, 1992.

Chang, T. P., Ko, H. H., Liu, F. J., Chen, P. H., Chang, Y. P., Liang, Y. H., Jang, H. Y., Lin, T. C. and Chen, Y. H.: Fractal dimension of wind speed time series. Appl. Energ., 93, 742-749, 2012.

Chiew, F., H., S. and McMahon, T., A.: Assessing the adequacy of catchment streamflow yield estimates. Soil Res. 31(5), 665-680, 1993.

560   Davis, A., Marshak, A., Wiscombe, W. and Cahalan, R.: Multifractal characterizations of nonstationarity and intermittency in geophysical fields: Observed, retrieved, or simulated. J. Geophys. Res.: Atmospheres, 99(D4), 8055-8072, 1994.

Deb, K.: Multi-Objective Optimization Using Evolutionary Algorithms. Chichester, England: John Wiley & Sons, 2001.

565   Demirel, M., C., Booij, M., J., and Hoekstra, A., Y.: Effect of different uncertainty sources on the skill of 10-day ensemble low flow forecasts for two hydrological models. Water Resour. Res. 49(7), 4035-4053, 2013.

Falconer, K.: Fractal geometry: mathematical foundations and applications. John Wiley & Sons, 2004.

Gao, Y., Leung, L., R., Zhang, Y. and Cuo, L.: Changes in moisture flux over the Tibetan Plateau

570   during 1979–2011: insights from a high-resolution simulation. J. Climate, 28(10), 4185-4197, 2015.

Grassberger, P. and Procaccia, I.: Measuring the strangeness of strange attractors. Physica D: Nonlinear Phenomena, 9(1-2), 189-208, 1983.

Gupta, H.V., Kling, H., Yilmaz, K.K. and Martinez, G.F.: Decomposition of the mean squared error

and NSE performance criteria: implications for improving hydrological modelling. J. Hydrol. 377 (1–2), 80–91, 2009.

Hao, Z. and Singh, V. P.: Entropy-based method for bivariate drought analysis. J. Hydrol. Eng., 18(7), 780-786, 2013.

Hurst HE: Long-term storage capacity of reservoirs. Trans. Am. Soc. Civil Eng. 116, 770–799, 1951.

Jain, S. and K., Sudheer, K., P.: Fitting of hydrologic models: a close look at the Nash–Sutcliffe index. J. Hydrol. Eng. 13(10), 981-986, 2008.

Karperien, A., Jelinek, H., F., Leandro, J., J., Soares, J., V., Cesar Jr, R. M., and Luckie, A.: Automated detection of proliferative retinopathy in clinical practice. Clinical ophthalmology (Auckland, NZ), 2(1), 109, 2008.

Katsev, S. and L'Heureux, I.: Are Hurst exponents estimated from short or irregular time series meaningful? Comput. Geosci. 29(9), 1085-1089, 2003.

Kling, H., Fuchs, M. and Paulin, M.: Runoff conditions in the upper Danube basin under an ensemble of climate change scenarios. J. Hydrol. 424, 264-277, 2012.

Krause, P., Boyle, D., P. and Baese, F.: Comparison of different efficiency criteria for hydrological model assessment. Adv. Geosci. 5, 89–97, 2005.

Kravchenko, A., N., Bullock, D., G. and Boast, C., W.: Joint multifractal analysis of crop yield and terrain slope. Agron. J., 92(6), 1279-1290, 2000.

Li, L., Xia, J., Xu, C. Y. and Singh, V. P.: Evaluation of the subjective factors of the GLUE method and comparison with the formal Bayesian method in uncertainty assessment of hydrological models. J. Hydrol., 390(3-4), 210-221, 2010.

Lindström, G., Johansson, B., Persson, M., Gardelin, M., and Bergström, S.: Development and test of the distributed HBV-96 hydrological model. J. Hydrol., 201, 272–288, 1997.

Liu, L., Gao, C., Xuan, W. and Xu, Y., P.: Evaluation of medium-range ensemble flood forecasting based on calibration strategies and ensemble methods in Lanjiang Basin, Southeast China. J. Hydrol. 554, 233-250, 2017.

Liu, L., Xu, Y. P., Pan, S. L., and Bai, Z.: Potential application of hydrological ensemble prediction in forecasting floods and its components over the Yarlung Zangbo River basin, China. Hydrol. Earth Syst.

Sc., 23(8), 3335-3352, 2019.

Mandelbrot, B., B.: A fractal set is one for which the fractal (Hausdorff-Besicovitch) dimension strictly exceeds the topological dimension. Fractals and Chaos. Springer, 2004.

605   Meseguer-Ruiz, O., Osborn, T. J., Sarricolea, P., Jones, P. D., Cantos, J. O., Serrano-Notivoli, R., and Martin-Vide, J.: Definition of a temporal distribution index for high temporal resolution precipitation data over Peninsular Spain and the Balearic Islands: the fractal dimension; and its synoptic implications. Clim. Dynam., 52(1-2), 439-456, 2019.

Movahed, M. S., and Hermanis, E.: Fractal analysis of river flow fluctuations. Physica A: Statistical

610   Mechanics and its Applications, 387(4), 915-932, 2008.

Nash, J., E., Sutcliffe, J., V., 1970. River flow forecasting through conceptual models part I—A discussion of principles. J Hydrol. 10(3), 282-290.

Onyutha, C., Rutkowska, A., Nyeko-Ogiramoi, P., and Willems, P.: How well do climate models reproduce variability in observed rainfall? A case study of the Lake Victoria basin considering CMIP3,

615   CMIP5 and CORDEX simulations. Stoch. Env. Res. Risk A. 33(3), 687-707, 2019.

Pan, S., Fu, G., Chiang, Y., M., Ran, Q., and Xu, Y., P.: A two-step sensitivity analysis for hydrological signatures in Jinhua River Basin, East China. Hydrologic. Sci. J. 62(15), 2511-2530, 2017.

Pan, S., Liu, L., Bai, Z., and Xu, Y., P.: Integration of Remote Sensing Evapotranspiration into Multi-Objective Calibration of Distributed Hydrology–Soil–Vegetation Model (DHSVM) in a Humid

620   Region of China. Water, 10, 1841, 2018.

Parra, V., Fuentes-Aguilera, P., and Muñoz, E.: Identifying advantages and drawbacks of two hydrological models based on a sensitivity analysis: a study in two Chilean watersheds. Hydrologic. Sc. J. 63(12), 1831-1843, 2018.

Pushpalatha, R., Perrin, C., Moine, and N., L., Andréassian, V.: A review of efficiency criteria suitable

625   for evaluating low-flow simulations. J. Hydrol. 420, 171-182, 2012.

Pechlivanidis, I. G., B. Jackson, H. McMillan, and H. Gupta: Use of an entropy-based metric in multiobjective calibration to improve model performance, Water Resour. Res., 50, 8066–8083, doi:10.1002/2013WR014537, 2014.

Radziejewski, M., and Kundzewicz, Z. W.: Fractal analysis of flow of the river Warta. J. Hydrology,

200(1-4), 280-294, 1997.

Rubalcaba, J. O.: Fractal analysis of climatic data: annual precipitation records in Spain. Theor. Appl. Climatol., 56(1-2), 83-87, 1997.

Seibert, J.: HBV Light, Version 2, User's Manual; Department of Physical Geography and Quaternary Geology, Stockholm University: Stockholm, Sweden, 2005.

Seibert, J., and Vis, M.: Teaching hydrological modeling with a user-friendly catchment-runoff-model software package. Hydrol. Earth Syst. Sc. 16, 3315–3325, 2012.

Shafii, M., and Tolson, B., A.: Optimizing hydrological consistency by incorporating hydrological signatures into model calibration objectives. Water Resour. Res, 51(5), 3796-3814, 2015.

Tian, Y., Xu, Y., Booij, M., J., and Cao, L.: Impact assessment of multiple uncertainty sources on high flows under climate change. Hydrol. Res. 47(1), 61-74, 2016.

Tian, Y., Xu, Y., Booij, M., J., and Wang, G.: Uncertainty in Future High Flows in Qiantang River Basin, China. J. Hydrometeorol. 16(1), 363-380, 2015.

Westerberg, I., K., and McMillan, H., K.: Uncertainty in hydrological signatures. Hydrol. Earth Syst. Sc. 19(9), 3951-3968, 2015.

Willems, P.: A time series tool to support the multi-criteria performance evaluation of rainfall-runoff models. Environ. Modell. Softw. 24(3), 311-321, 2009.

Yu, Z., G., Leung, Y., Chen, Y., D., Zhang, Q., Anh, V., and Zhou, Y.: Multifractal analyses of daily rainfall time series in Pearl River basin of China. Physica A: Statistical Mechanics and its Applications, 405, 193-202, 2014.

Zhang, Q., Yu, Z., G., Xu, C., Y., and Anh, V.: Multifractal analysis of measure representation of flood/drought grade series in the Yangtze Delta, China, during the past millennium and their fractal model simulation. Int. J. Climatol. 30(3), 450-457, 2010.

Zhou, Y., Zhang, Q., and Singh, V., P.: Fractal-based evaluation of the effect of water reservoirs on hydrological processes: the dams in the Yangtze River as a case study. Stoch. Env. Res. Risk A. 28(2), 263-279, 2014.

Zhu, Q., Gao, X., Xu, Y., P., and Tian, Y.: Merging multi-source precipitation products or merging their simulated hydrological flows to improve streamflow simulation. Hydrologic. Sci. J., 64(8), 910-

920, 2019.

660 **Table 1: Comparison of best E between single-objective calibration and multi-objective calibration (E-RD strategy).**

	Single-objective (E)	Multi-objective (E)
Dong	0.696	0.690
Jinhua	0.951	0.953
Xiang	0.820	0.822

Table 2: Hydrological signatures of typical models in all three cases.

		Observation	Best RD	Best E	Largest RD
Auto correlation	Dong	0.97	0.99	1.00	1.00
	Jinhua	0.76	0.76	0.76	0.75
	Xiang	0.94	0.95	0.94	0.94
Relative variance	Dong	0.53	0.56	0.58	0.57
	Jinhua	1.87	1.87	1.87	1.89
	Xiang	0.99	0.82	0.92	0.92
Maximum monthly flow (m^3/s)	Dong	1.54	1.40	1.42	1.39
	Jinhua	531.19	497.40	503.68	496.77
	Xiang	4210.01	3956.24	4027.68	4042.94
Minimum monthly flow (m^3/s)	Dong	0.44	0.30	0.27	0.26
	Jinhua	60.64	58.85	50.45	60.19
	Xiang	961.00	975.07	812.02	840.02
High flow percentiles $(Q_5)(m^3/s)$	Dong	1.93	1.44	1.49	1.38
	Jinhua	752.00	745.02	734.12	740.28
	Xiang	6048.50	5817.06	5586.92	5817.08
low flow percentiles $(Q_{75})(m^3/s)$	Dong	0.50	0.39	0.40	0.38
	Jinhua	37.77	38.55	37.80	37.31
	Xiang	803.75	790.95	845.76	744.52

665

Table 3: Determinative parameters and distance correlations (r_d^2) between parameters and RD. *: $r_d^2 \geq 0.8$

	r_d^2 (range of parameter)		
	Dong	Jinhua	Xiang
Effective precipitation exponent (β) (mm/mm)	0.363 (0.010~0.012)	0.709 (0.791~0.911)	0.739 (0.435~0.499)
Fast flow exponent (α)	0.383 (0.100~0.124)	*0.808 (0.473~0.579)	0.734 (0.677~0.819)
Fast flow factor (KF)	*0.853 (0.002~0.005)	*0.812 (0.031~0.056)	*0.823 (0.003~0.006)
Baseflow factor (KS)	*0.932 (0.016~0.153)	*0.922 (0.005~0.063)	*0.950 (0.010~0.048)
Percolation (mm/day)	*0.879 (1.37~7.00)	*0.841 (1.10~2.34)	*0.959 (1.62~3.16)
Capillary transport (mm/day)	0.122 (0~0.035)	0.084 (3.84~4.00)	*0.914 (1.91~2.70)
Degree-day factor (mm/(day ℃))	0.117 (0.01~12.2)	0.171 (14.5~15.6)	*0.791 (2.80~4.20)

670

Table 4 Parameters of WETSPRO.

Parameter	Dong	Jinhua	Xiang
Recession constant (days)	90	80	90
w-parameter filter	0.14	0.43	0.38

675

$\delta = 128, \quad N = 3$

$\delta = 64, \quad N = 8$

$\delta = 32, \quad N = 19$
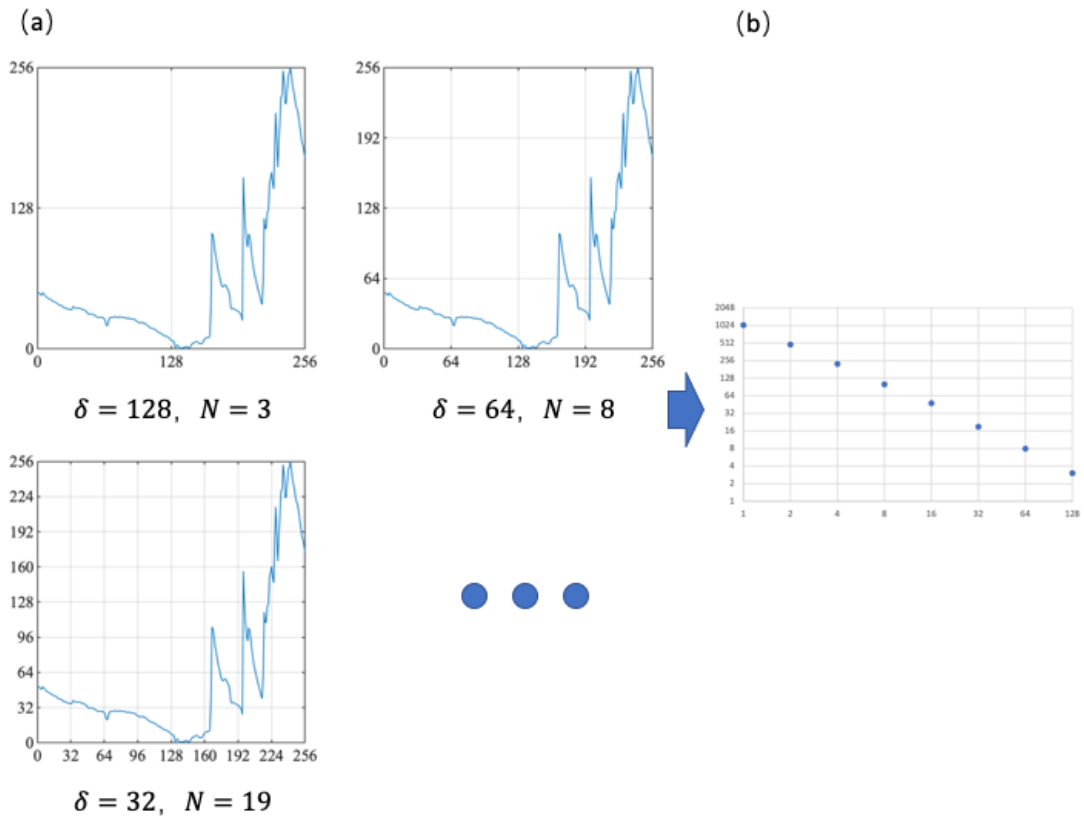
Figure 1: Flow chart of using box-counting method to calculate the Hausdorff dimension of time series.

680
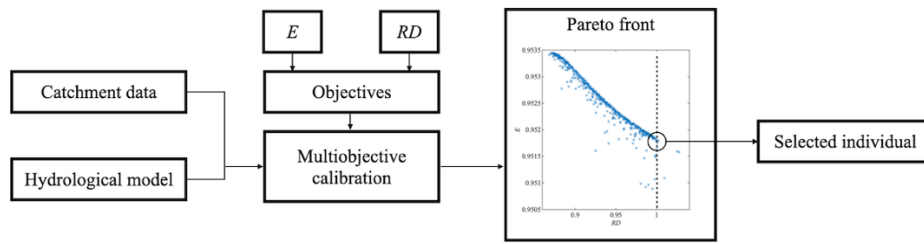
Figure 2: Flow chart of *E-RD* strategy.
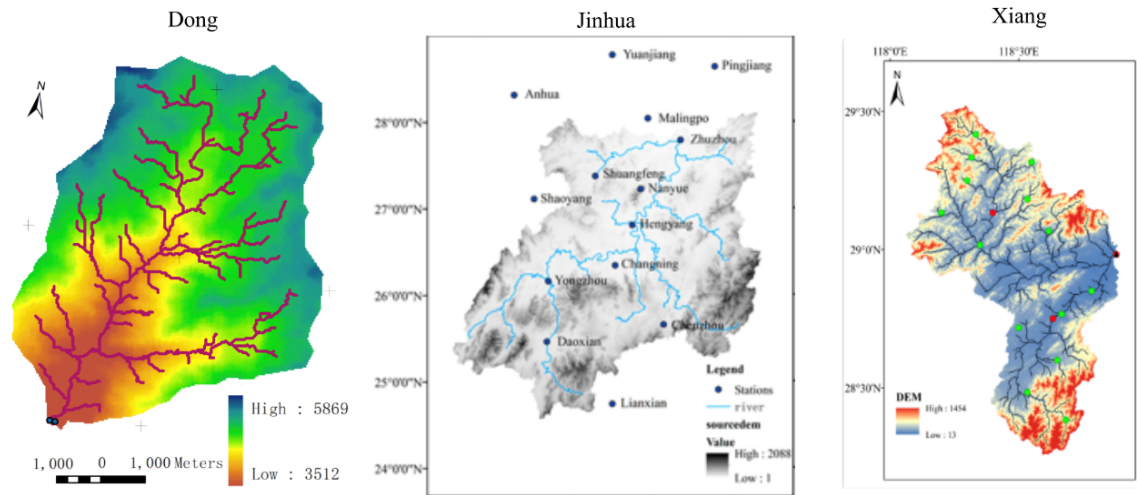
685 **Figure 3:DEM of study areas.**
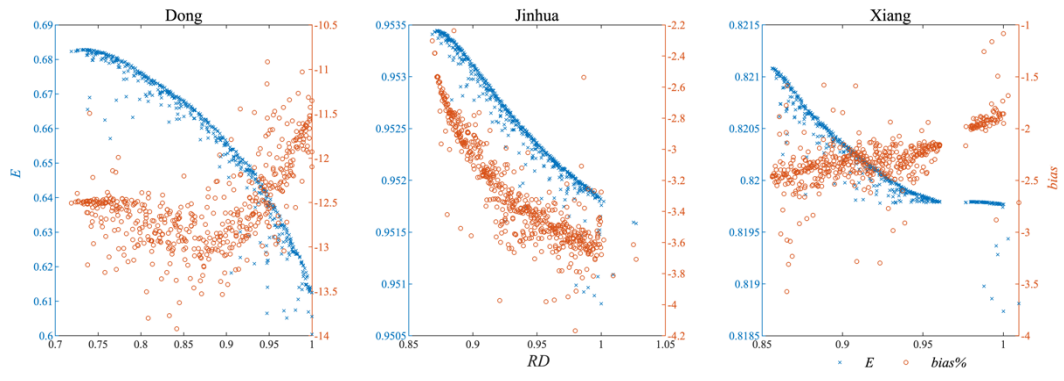
690   **Figure 4:** *E-RD* **of last generation of GA calibration.**
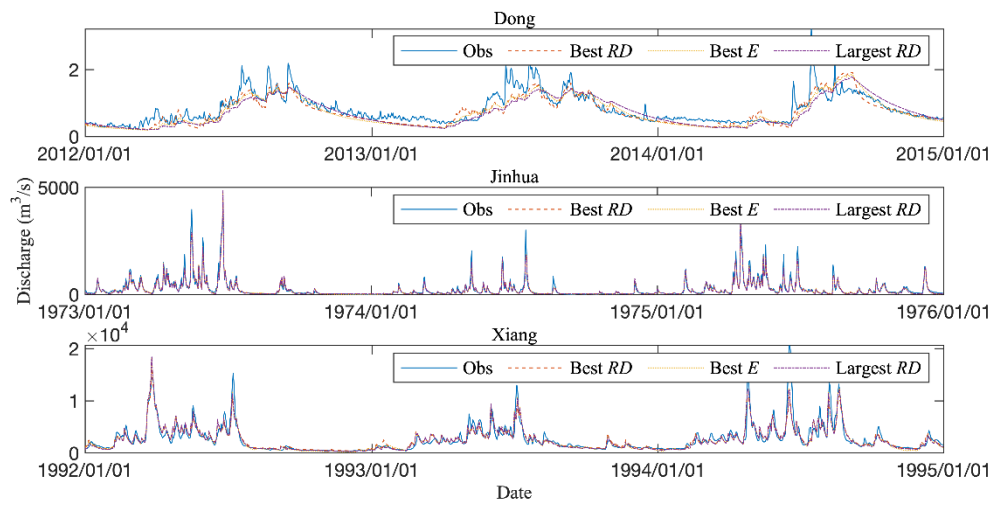
Figure 5: Typical examples with best *RD*, best *E* and largest *RD* (representative three-year hydrograph).
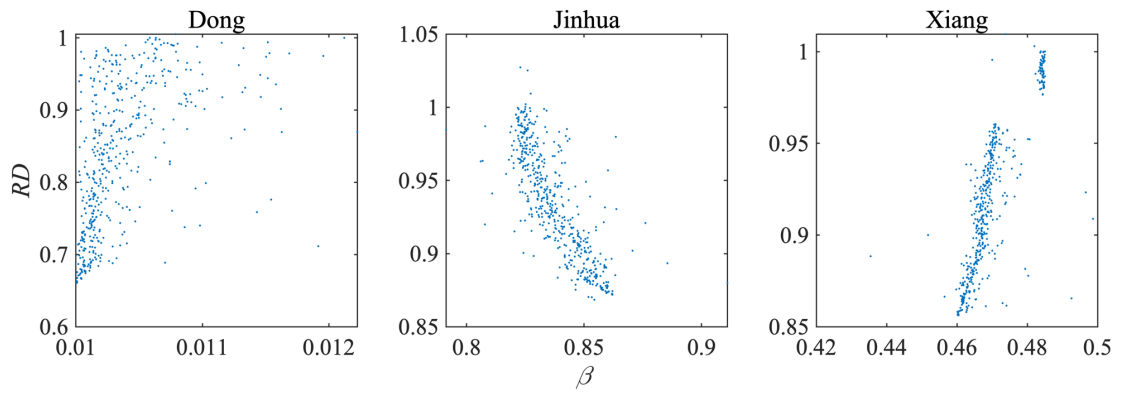
Figure 6:β and RD relationship in three cases.

700
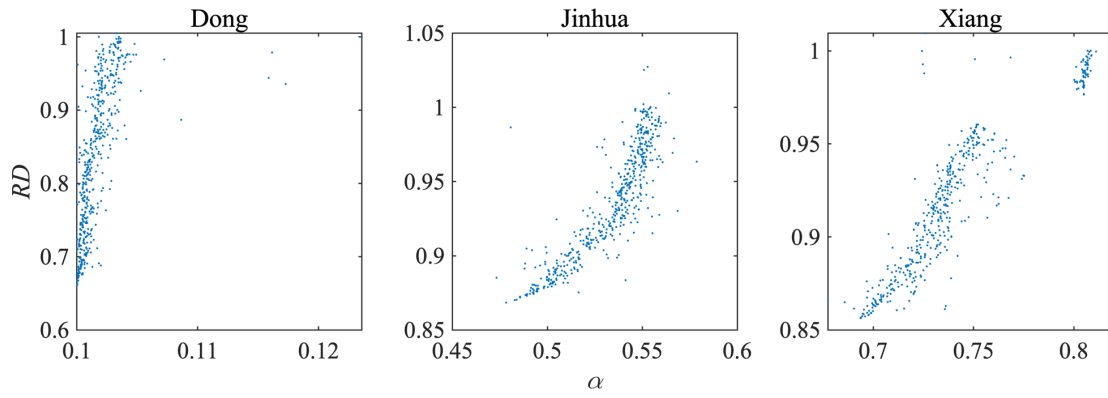
Figure 7: α and RD relationship in three cases.
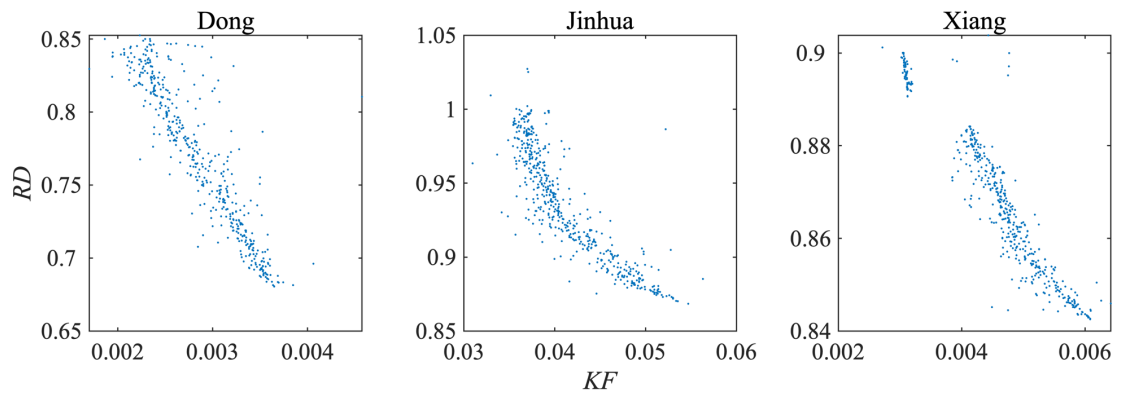
705

Figure 8: KF and *RD* relationship in three cases.
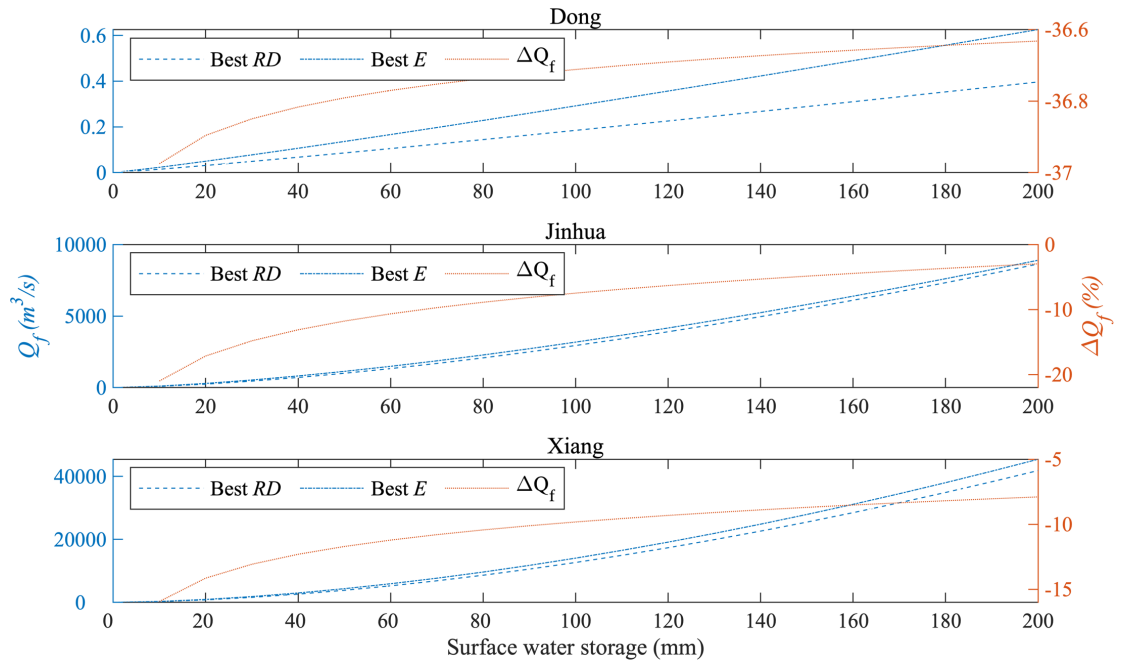
Figure 9: Response of fast flow to surface water storage. For each case, fast flow responses of typical models with best *RD* and *E* are presented.
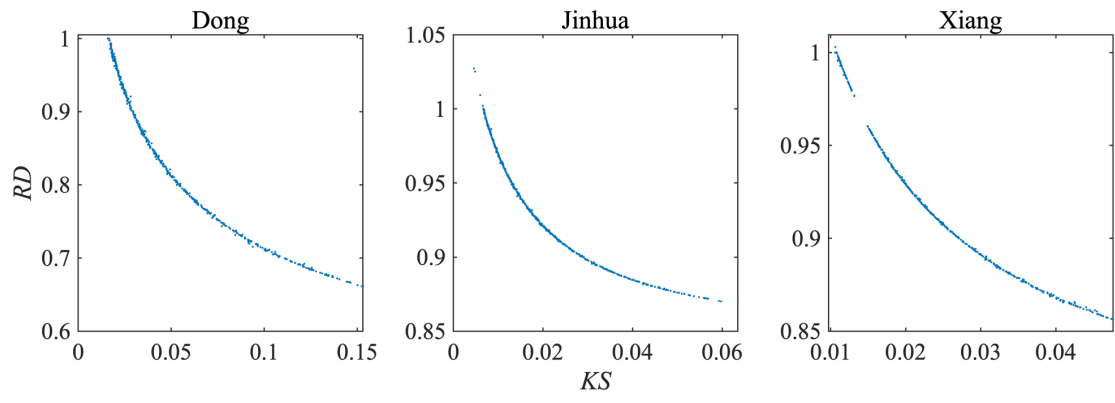
Figure 10:KS and *RD* relationship in three cases.
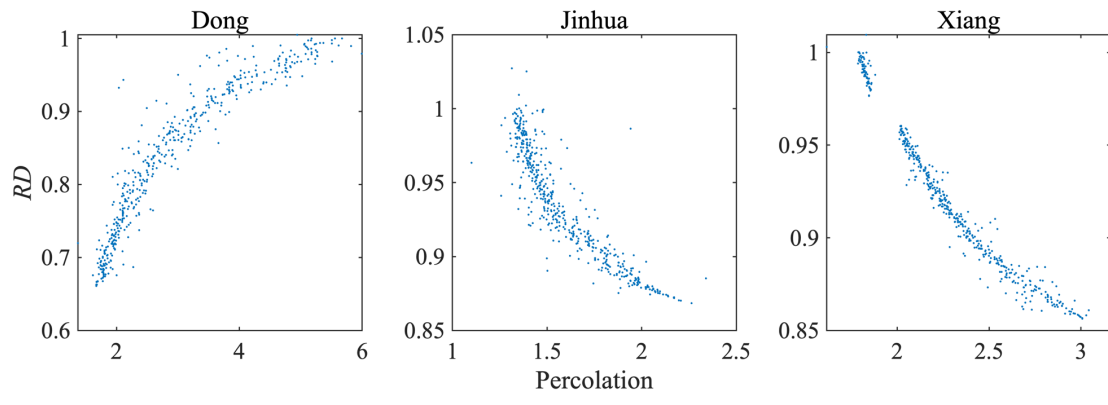
715

Figure 11: Percolation and *RD* relationship in three cases.
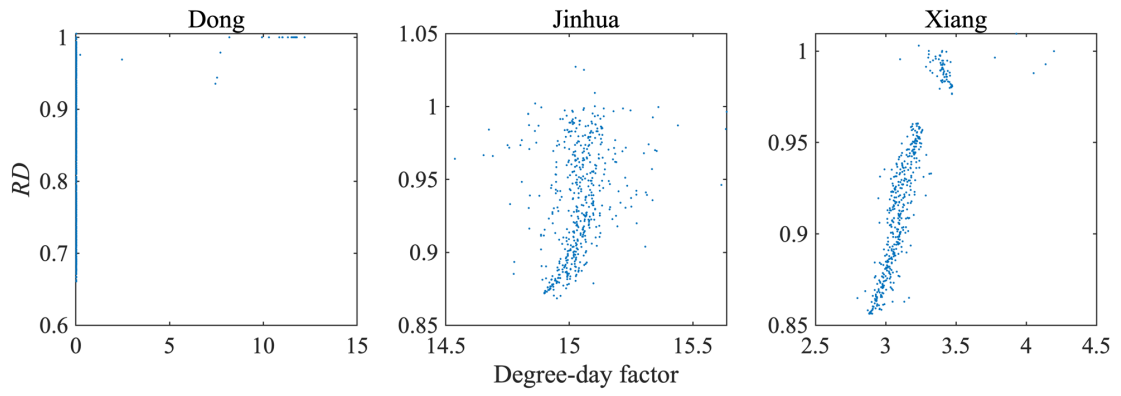
Figure 12:Degree-day factor and *RD* relationship in three cases.

720
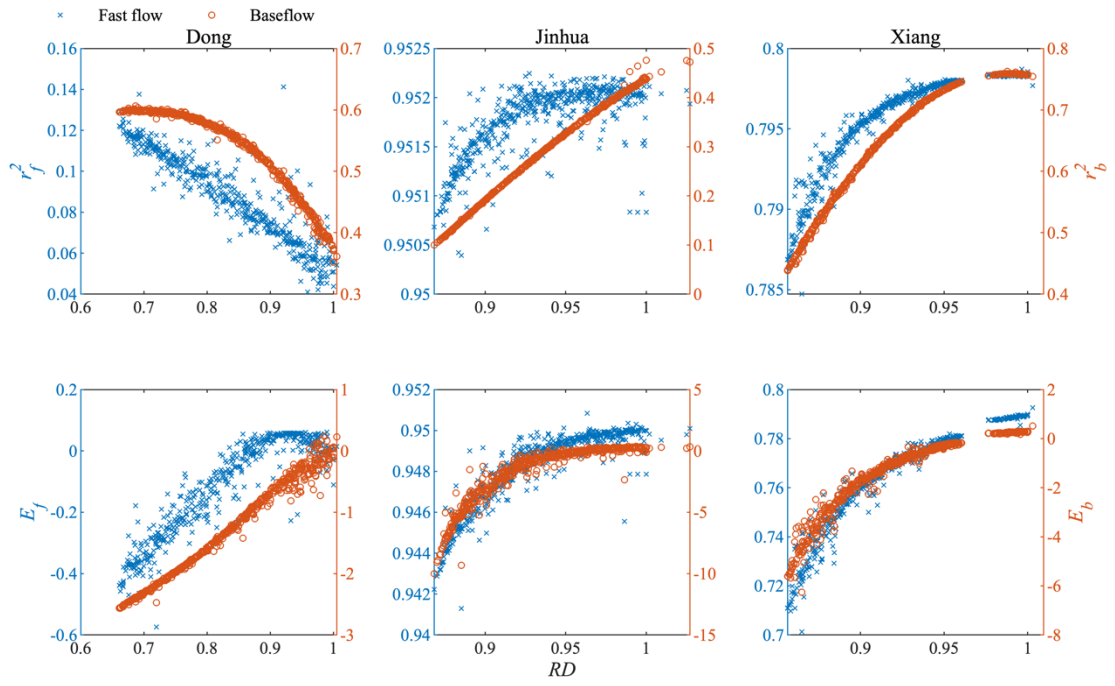
Figure 13: Correlation coefficients and Nash-Sutcliffe efficiency coefficients on fast flow and baseflow respectively of models of last generation in three cases.
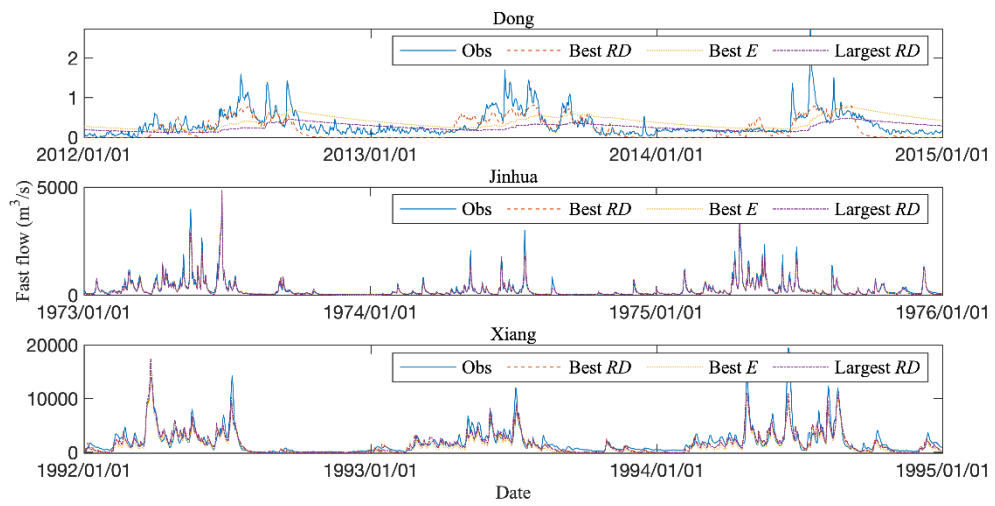
725

Figure 14: Fast flow of typical models and observations (representative three-years hydrograph).
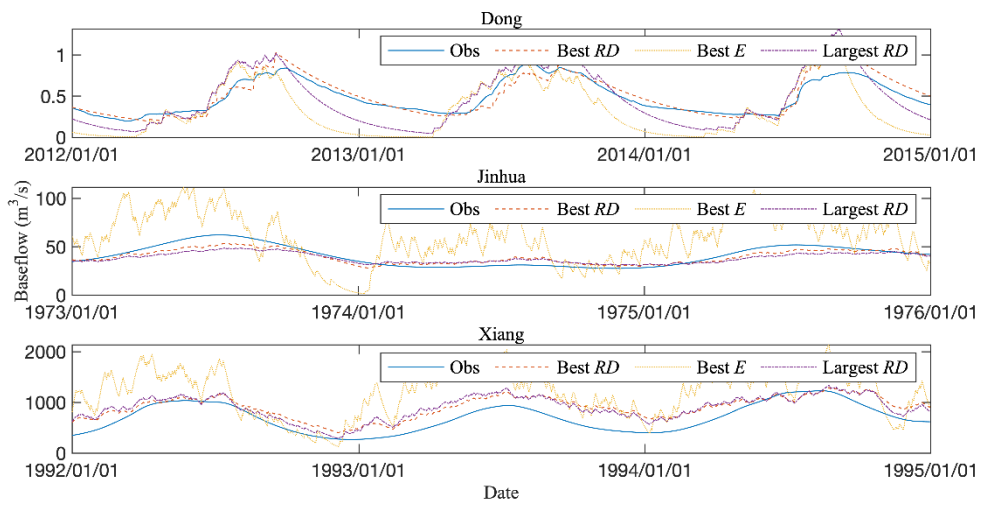
Figure 15: Baseflow of typical models and observations (representative three-years hydrograph).

730